

Light scattering from a degenerate quasi-one-dimensional confined gas of non-interacting fermions

Patrizia Vignolo, Anna Minguzzi and M. P. Tosi

Istituto Nazionale di Fisica della Materia and Classe di Scienze, Scuola Normale Superiore, Piazza dei Cavalieri 7, I-56126 Pisa, Italy

We evaluate the scattering functions of a gas of spin-polarized, non-interacting fermions confined in a quasi-one-dimensional harmonic trap at zero temperature. The main focus is on the inelastic scattering spectrum and on the angular distribution of scattered light from a mesoscopic atomic cloud as probes of its discrete quantum levels and of its shell structure in this restricted geometry. The dynamic structure factor is calculated and compared with the results of a local-density approximation exploiting the spectrum of a one-dimensional homogeneous Fermi gas. The elastic and inelastic contributions to the static structure factor are separately evaluated: the inelastic term becomes dominant as the momentum transfer increases, masking a small peak at twice the Fermi momentum in the elastic term but still reflecting the discrete quantum levels of the cloud. A fast and accurate numerical method is developed to evaluate the full pair distribution function for mesoscopic inhomogeneous clouds.

PACS numbers: 05.30.Fk,32.90.+a

I. INTRODUCTION

There currently is considerable experimental activity in trapping and cooling dilute gases of the fermionic alkali atoms ^{40}K [1] and ^6Li [2] in the quantum degeneracy regime. A quasi-one-dimensional (quasi-1D) and almost ideal neutral Fermi gas can be realized in these experiments by using a very anisotropic, cigar-shaped magnetic trap. In this arrangement the fermionic atoms can be placed into a single Zeeman sublevel, yielding a spin-polarized state in which their mutual interactions are extremely weak [3,4], and are subject to approximately harmonic confinement in the axial direction and to tight confinement in the other directions.

The possibility of experimentally studying such a close realization of an ideal 1D Fermi gas in harmonic external potential presents great interest for the theory of quantum gases. To begin with, the 1D model of non-interacting fermions has the same particle density profile and thermodynamic and dynamic properties as the 1D model of point-like bosons with hard-core interactions [5]. Given this wider relevance of the model, harmonic confinement is probably the simplest way to realize an inhomogeneous quantum fluid on which to test the ideas and the implementations of Density Functional Theory [6]. Of specific interest in the present context is the kinetic energy functional, which can be constructed exactly from the particle density in the case of N fermions moving independently in a harmonic oscillator potential [7]. Finally, the shell structure that was noticed in the particle density of the Fermi gas in 3D [8] is greatly enhanced in lower dimensionality [9,10]. Very efficient numerical methods have been developed [9,11] to evaluate ground-state properties of mesoscopic 1D clouds containing large numbers of fermions.

The present work completes our earlier study of the ideal 1D Fermi gas under harmonic confinement [9,11] by evaluating the spectral properties of low-frequency radiation scattered from its quasi-1D realization. Previous studies of the scattering spectrum of the homogeneous ideal Fermi gas [12,13] and of the off-resonant light scattering properties of an ideal Fermi gas under isotropic harmonic confinement [3] have referred to the 3D case. Our objective is to examine how the shell structure of the particle density profile and the single occupancy of discrete quantum levels in this specific quasi-1D geometry are reflected in the light-scattering properties and, at a deeper level, how the shell structure appears in the pair distribution function as a gauge of the spatial correlations induced by the Pauli exclusion principle between pairs of fermions.

The layout of the paper is briefly as follows. In Sections II and III we recall from the work of Javanainen and Ruostekoski [13] the basic facts about light scattering from an atomic cloud and explicitly set out how the inelastic scattering spectrum and the angular distribution of the scattered light are related to the time-dependent pair distribution function. In Sec. IV we present an evaluation of the dynamic structure factor of a mesoscopic Fermi gas in harmonic confinement and compare its results with those obtained from a local-density approximation (LDA) exploiting the spectrum of the homogeneous gas. Section V evaluates both the elastic and the inelastic contribution to the static structure factor, again comparing the latter results with the LDA. In Sec. VI we present numerical results for the equal-times pair distribution function, which are obtained by an extension of the Green's function method previously developed [9] for the one-body density matrix. Finally, Sec. VII summarizes our main conclusions.

II. LIGHT SCATTERING FROM AN ATOMIC CLOUD

We consider a confined cloud of spin-polarized, magnetically trapped atoms in a quasi-1D configuration. We focus on a light scattering experiment with the incident beam propagating along the z axis, orthogonal to the x axis which is the axial direction of the magnetic trap (see Fig. 1). The positive-frequency component of the incident electric field is

$$\mathbf{E}_F^+(z, t) = \frac{1}{2} \mathcal{E} \hat{\epsilon} e^{i(k_L z - \omega_L t)}, \quad (1)$$

where \mathcal{E} is the field amplitude, $\hat{\epsilon}$ is the polarization, k_L and ω_L are the light wave number and frequency. In regard to the internal states we model each atom as a two-level system, *i.e.* an excited state $|e\rangle$ and a ground state $|g\rangle$ separated by an energy $\hbar\omega_A$. This corresponds to a suitable choice of the Zeeman sublevel for the atoms in the ground state and, at the same time, of the light polarization. Angular momentum degeneracy of the internal states in the case of an unpolarized cloud has been treated by Javanainen and Ruostekoski [13].

In the Born approximation the scattered light at a point on the screen designated by the vector \mathbf{R} (see again Fig. 1) is given by [13]

$$\mathbf{E}_S^+(\mathbf{R}, t) = \mathcal{E} \frac{k_L^2}{8\pi\epsilon_0\hbar\delta} \frac{e^{ik_L R}}{R} [\hat{n} \times (\hat{n} \times \mathbf{d}^-)] (\hat{\epsilon} \cdot \mathbf{d}^+) \int_{\text{cloud}} d^3 r' e^{-i\mathbf{k} \cdot \mathbf{r}'} \hat{\psi}^\dagger(\mathbf{r}', t) \hat{\psi}(\mathbf{r}, t). \quad (2)$$

Here $\delta = \omega_L - \omega_A$ is the detuning between the laser frequency and the atomic transition, $\hat{n} = \mathbf{R}/R$, $\mathbf{d}^+ = \mathcal{D} \hat{\epsilon} |e\rangle\langle g|$ and $\mathbf{d}^- = \mathcal{D} \hat{\epsilon} |g\rangle\langle e|$ are the raising and lowering parts of the dipole-moment operator of amplitude \mathcal{D} , $\mathbf{k} = k_L \hat{n} - \mathbf{k}_L$ is the wave vector transfer and \mathbf{r}' indicates an atom in the cloud (see Fig. 1). Finally, $\hat{\psi}(\mathbf{r}, t)$ is the annihilation field operator for atoms in the internal state $|g\rangle$.

The spectrum of scattered radiation from atoms in the ground state at the point \mathbf{R} is

$$\mathcal{I}(\mathbf{k}, \omega) = \frac{1}{2\pi} M(\hat{\epsilon}, \hat{n}) I(R) \frac{\Omega^2}{\delta^2} \int dt \int d^3 r_1 \int d^3 r_2 e^{i(\omega t - \mathbf{k} \cdot (\mathbf{r}_1 - \mathbf{r}_2))} \langle \hat{\psi}^\dagger(\mathbf{r}_1, t) \hat{\psi}(\mathbf{r}_1, t) \hat{\psi}^\dagger(\mathbf{r}_2, 0) \hat{\psi}(\mathbf{r}_2, 0) \rangle. \quad (3)$$

Here $M(\hat{\epsilon}, \hat{n}) = (1 + \cos^2(\theta))/2$ is the geometric factor for detection at an angle θ in the case of circularly polarized light; $I(R) = \mathcal{D}^2 \omega_L^2 / (32\pi^2 \epsilon_0 c^3 R^2)$ is the total intensity scattered by a single dipole, and $\Omega = \mathcal{D}\mathcal{E}/(2\hbar)$ is the Rabi frequency. The triple integral on the RHS of Eq. (3) at $\omega \neq 0$ is the dynamic structure factor $S(\mathbf{k}, \omega)$ for inelastic scattering.

The angular distribution of the scattered light is

$$\mathcal{I}(\mathbf{k}) = \int d\omega \mathcal{I}(\mathbf{k}, \omega), \quad (4)$$

the angular dependence being implicit in the direction of \mathbf{k} . The distribution of scattered light can be decomposed into two components: an elastic term, originating from the diffraction of the light by a finite object of given density profile, and an inelastic term determined by the excitations of the quantum fluid.

III. GENERAL DEFINITIONS

According to Eq. (3) the microscopic quantity which is relevant for the spectrum of scattered light is the time-dependent pair distribution function,

$$\rho_2(1, 2) = \langle \hat{\psi}^\dagger(1) \hat{\psi}(1) \hat{\psi}^\dagger(2) \hat{\psi}(2) \rangle. \quad (5)$$

Here we have set (1) = (\mathbf{r}_1, t_1) and (2) = (\mathbf{r}_2, t_2) . For a non-interacting Fermi gas the expansion of the field operators into energy modes \hat{a}_i , that is $\hat{\psi}(1) = \sum_i \phi_i(\mathbf{r}_1) \exp(-i\varepsilon_i t_1) \hat{a}_i$, yields an explicit expression for the pair distribution function in terms of the single-particle orbitals $\phi_i(\mathbf{r})$:

$$\begin{aligned} \rho_2(1, 2) &= \sum_{i,j} \phi_i^*(\mathbf{r}_1) \phi_j(\mathbf{r}_1) \phi_j^*(\mathbf{r}_2) \phi_i(\mathbf{r}_2) e^{-i(\varepsilon_j - \varepsilon_i)(t_1 - t_2)/\hbar} f(\varepsilon_i) [1 - f(\varepsilon_j)] + n(1)n(2) \\ &\equiv S(1, 2) + n(1)n(2), \end{aligned} \quad (6)$$

where $n(1)$ is the equilibrium density profile and $f(\varepsilon)$ is the Fermi distribution function.

The dynamic structure factor is given by

$$\begin{aligned} S(\mathbf{k}, \omega) &= \int dt \int d^3 r_1 \int d^3 r_2 e^{i[\omega t - \mathbf{k} \cdot (\mathbf{r}_1 - \mathbf{r}_2)]} S(1, 2)|_{t=t_1-t_2} \\ &= \sum_{i,j} \left| \int d^3 r e^{-i\mathbf{k} \cdot \mathbf{r}} \phi_i^*(\mathbf{r}) \phi_j(\mathbf{r}) \right|^2 f(\varepsilon_i) [1 - f(\varepsilon_j)] 2\pi \delta(\omega - (\varepsilon_j - \varepsilon_i)/\hbar). \end{aligned} \quad (7)$$

By integration over frequency one obtains the inelastic contribution to the static structure factor:

$$\begin{aligned} S_i(\mathbf{k}) &\equiv \int \frac{d\omega}{2\pi} S(\mathbf{k}, \omega) \\ &= \int d^3 r_1 \int d^3 r_2 e^{-i\mathbf{k} \cdot (\mathbf{r}_1 - \mathbf{r}_2)} [\rho_2(\mathbf{r}_1, \mathbf{r}_2) - n(\mathbf{r}_1)n(\mathbf{r}_2)]. \end{aligned} \quad (8)$$

Here $\rho_2(\mathbf{r}_1, \mathbf{r}_2)$ is the equal-times pair distribution function, which for non-interacting fermions can be expressed as

$$\rho_2(\mathbf{r}_1, \mathbf{r}_2) = n(\mathbf{r}_1)\delta(\mathbf{r}_1 - \mathbf{r}_2) - \rho_1(\mathbf{r}_1, \mathbf{r}_2)\rho_1(\mathbf{r}_2, \mathbf{r}_1) + n(\mathbf{r}_1)n(\mathbf{r}_2), \quad (9)$$

where $\rho_1(\mathbf{r}_1, \mathbf{r}_2) = \langle \hat{\psi}^\dagger(\mathbf{r}_1)\hat{\psi}(\mathbf{r}_2) \rangle$ is the one-body Dirac density matrix.

The next sections will be devoted to the evaluation of these quantities in a quasi-1D Fermi gas under harmonic confinement $V_{ext}(\mathbf{r}) = m\omega_{ho}^2[x^2 + \lambda^2(y^2 + z^2)]/2$, that is, a Fermi gas in a cigar-shaped harmonic trap where $\lambda \gg 1$ and only the values $n_y = 0$ and $n_z = 0$ of the transverse quantum numbers are allowed. For simplicity we choose $\hbar = 1$, $m = 1$ and $\omega_{ho} = 1$.

IV. DYNAMIC STRUCTURE FACTOR

The transverse excited states are not involved in the excitation processes when (i) the transverse component k_\perp of the momentum transfer vanishes, due to orthogonality of harmonic oscillator wave functions, or (ii) the energy transfer ω is smaller than the gap between the chemical potential and the first transverse excited state. In these limits Eq. (7) reduces to a one-dimensional problem and the transverse-state wave function factorizes out. Following De Marco and Jin [3] we evaluate the overlap integral $I = \int dx_1 \exp(ik_x x_1) \phi_i^*(x_1) \phi_j(x_1)$ in momentum space to obtain

$$I = \int \frac{dq}{2\pi} \tilde{\phi}_i^*(q + k_x/2) \tilde{\phi}_j(q - k_x/2), \quad (10)$$

where $\tilde{\phi}_i(p) = \mathcal{H}_i(p) \exp(-p^2/2)/\pi^{1/4}\sqrt{2^i i!}$. By exploiting the properties of the Hermite polynomials $\mathcal{H}_i(p)$ [14], we finally obtain the expression for the dynamic structure factor as

$$S(\mathbf{k}, h) = 2\pi e^{-k_\perp^2/2\lambda} e^{-k_x^2/2} \sum_{i=\max\{N-h, 0\}}^{N-1} \frac{i!}{(i+h)!} \left(\frac{k_x^2}{2}\right)^h [L_i^h(k_x^2/2)]^2. \quad (11)$$

Here h is an integer corresponding to a single-atom excitation of h quanta of the harmonic oscillator and $L_i^h(x)$ is the i^{th} generalized Laguerre polynomial of parameter h . The spectrum in Eq. (11) is discrete due to the external harmonic confinement, but can of course be approximated as a continuum in the limit $\omega \gg \omega_{ho}$. Figure 2 illustrates the spectrum at various numbers of particles, for two values of the transferred wave vector in the x direction.

The main qualitative features of the spectrum can be understood within a local-density description, which exploits the results for the dynamic structure factor $S_{hom}(k_x, \omega)$ of the homogeneous 1D system in a medium with a locally varying density profile $n(x)$ to predict the spectrum of a strictly 1D system as

$$S_{LDA}(k_x, \omega) = \int dx n(x) S_{hom}(k_x, \omega; \mu(x)). \quad (12)$$

The spatial dependence of the chemical potential $\mu = k_F^2/2 = \pi^2 n^2/2$ is determined by the relation $\mu(x) = \mu(n(x))$. In the case of external harmonic confinement we use the expression for the homogeneous 1D Fermi gas,

$$S_{hom}(k_x, \omega) = \begin{cases} \pi/k_x k_F & \text{if } |\omega_2(k_x)| < \omega < \omega_1(k_x) \\ 0 & \text{otherwise} \end{cases} \quad (13)$$

where $\omega_{1,2} = k_x^2/2 \pm k_x k_F$, together with the density profile in LDA,

$$n(x) = \frac{1}{\pi} \sqrt{2N - x^2} \quad (14)$$

to obtain the dynamic structure factor:

$$S_{LDA}(k_x, \omega) = \frac{2}{k_x} \left[\sqrt{2N - \left(\frac{\omega}{k_x} - \frac{k_x}{2}\right)^2} - \sqrt{2N - \left(\frac{\omega}{k_x} + \frac{k_x}{2}\right)^2} \right]. \quad (15)$$

The LDA curves for the dynamic structure factor are also shown in Fig. 2, together with the spectrum of the homogeneous gas. Evidently, the effect of the confinement is to change very substantially the spectrum with respect to the homogeneous case, and the general spectral shape is well described within a local-density picture.

V. ANGULAR DISTRIBUTION OF THE SCATTERED LIGHT

The angular distribution of the scattered radiation is related through Eqs. (3) and (4) to the equal-times pair distribution function. Both an elastic term and an inelastic term contribute to its expression: the former is related to the particle-density profile of the cloud while the latter arises from the internal excitations of the cloud.

A. Elastic contribution

The elastic contribution to the diffraction pattern of a quasi-1D gas is given by

$$S_e(\mathbf{k}) = e^{-k_{\perp}^2/2\lambda} \left| \int dx e^{-ik_x x} n(x) \right|^2. \quad (16)$$

In evaluating this term, which is of order N^2 , we have looked for the effect of the shell structure of the density profile on the angular distribution of the scattered light.

With this aim, we have compared the Fourier Transform (FT) $\tilde{n}(k_x)$ of the 1D density profile with its LDA expression, which can be evaluated in terms of the Bessel function J_1 as [10]

$$\tilde{n}_{LDA}(k_x) = \frac{\sqrt{2N}}{k_x} J_1(\sqrt{2N}k_x). \quad (17)$$

The same behaviour is found for these two curves in the central peak of the diffraction pattern (Fig. 3(a)), where the dominant contribution is due to the finite size of the cloud. The FT of the exact profile differs instead from that of the LDA (Thomas-Fermi) profile in that it contains a side peak at a value $k_x \simeq 2\pi/\Delta x$ of the transferred momentum, where Δx is the average distance between two nearest maxima in the shell structure. An estimate of Δx can be made by taking the maxima to be uniformly distributed along the LDA profile, yielding

$$\Delta x \simeq \frac{2R_{LDA}}{N} = \frac{2\sqrt{2}a_{ho}}{\sqrt{N}}, \quad (18)$$

where R_{LDA} is the axial Thomas Fermi radius of the cloud. For $N=100, 500$ and 1000 we have recognized this side peak in the diffraction pattern (see Fig. 3(b) for $N=100$). As noticed earlier [10] its position corresponds to $k_x \simeq 2k_F$. However, the relative intensity of the peak is extremely weak and as we expected it decreases with increasing N , as the density profile gets closer to the Thomas-Fermi one. At higher values of the momentum transfer the elastic contribution to the diffraction pattern approximately vanishes, while the Thomas-Fermi pattern has an oscillating tail which still reflects the finite extension of the profile in space.

The total distribution of the scattered light is the sum of the elastic and inelastic contributions: while for small values of k_x the elastic contribution is dominant but does not distinguish between the true and the Thomas-Fermi profile, the inelastic contribution overcomes it at finite values of k_x . This is shown immediately below. It is thus very difficult to resolve the specific effect of the shell structure by this method.

B. Inelastic contribution: the static structure factor

The inelastic contribution to the intensity of scattered radiation is obtained from the static structure factor in Eq. (8). This contribution is proportional to the number N of particles in the sample. In the case of quasi-1D harmonic confinement, by the same procedure which has led to Eq. (11) we obtain an analytic expression for $S_i(\mathbf{k})$ in terms of the generalized Laguerre polynomials:

$$S_i(\mathbf{k}) = N - e^{-k_\perp^2/2\lambda} e^{-k_x^2/2} \sum_{i,j=0}^{N-1} \frac{i!}{j!} \left(\frac{k_x^2}{2}\right)^{j-i} \left[L_i^{j-i}(k_x^2/2)\right]^2. \quad (19)$$

In Figure 4 we show the function $S_i(\mathbf{k})$ at $k_\perp = 0$ for various values of the particle number N . The condition $k_\perp \simeq 0$ applies to small angles in Fig. 1. The quantum effect of single-level occupancy in the external potential is most visible in the first derivative of $S_i(k_x)$, as is shown in the inset in Fig. 4.

The local-density result, obtained by integration of the 1D Eq. (15) yields the following expression for a strictly 1D system:

$$S_{LDA}(k_x) = \begin{cases} \left[2N \text{ArcTan}(k_x/\sqrt{8N - k_x^2}) + k_x \sqrt{8N - k_x^2}/4\right] / \pi & \text{if } k_x < 2\sqrt{2N} \\ N & \text{if } k_x \geq 2\sqrt{2N}. \end{cases} \quad (20)$$

It follows from the discussion in Sec. IV that the 1D LDA provides a good description of the structure factor at $k_\perp = 0$ as N increases. In fact, although the LDA does not take shell effects into account, it gives the general behavior of $S_i(k_x)$ already for small numbers of fermions ($N \geq 20$). The LDA curve has not been shown in Fig. 4 since it is indistinguishable from the $N = 100$ result.

VI. EQUAL-TIMES PAIR DISTRIBUTION FUNCTION

Because of its definition as a double space integral in Eq. (8), the inelastic term in the static structure factor displays only part of the information which is contained in the equal-times pair distribution function $\rho_2(\mathbf{r}_1, \mathbf{r}_2)$ as defined in Eq. (9). In this section we give a full evaluation of this function for the quasi-1D gas of present interest. Our main objective will be to explicitly show how $\rho_2(\mathbf{r}_1, \mathbf{r}_2)$ reflects the Pauli exclusion principle and the shell structure of the fermion cloud. The same results apply to a 1D Bose gas with hard-core interactions, since the boson-fermion mapping holds for the equal-times pair distribution function [15].

With the notation $\phi_\perp(y, z)$ for the transverse ground-state wave function of the quasi-1D system of non-interacting fermions in the external confining potential, we can write the pair distribution function as

$$\rho_2(\mathbf{r}_1, \mathbf{r}_2) = n(\mathbf{r}_1)\delta(\mathbf{r}_1 - \mathbf{r}_2) - w(\mathbf{r}_{1\perp}, \mathbf{r}_{2\perp}) [F(x_1, x_2) - n(x_1)n(x_2)] \quad (21)$$

where $r_\perp = (y, z)$ and $w(\mathbf{r}_{1\perp}, \mathbf{r}_{2\perp}) = |\phi_\perp(y_1, z_1)|^2 |\phi_\perp(y_2, z_2)|^2$. The function $F(x_1, x_2)$ is given by

$$F(x_1, x_2) = \sum_{i,j=1}^N \phi_i^*(x_1)\phi_j(x_1)\phi_j^*(x_2)\phi_i(x_2) \quad (22)$$

and will be calculated below by an efficient numerical method based on an extension of the Green's function method used previously [9,11] to evaluate particle and kinetic energy densities. Direct calculation can be used for limited numbers of fermions [15], but the present method is easily applied to handle mesoscopic clouds containing a large number of fermions.

A. Method

We first rewrite Eq. (22) in terms of the Green's function $\hat{G}(x) = (x - \hat{x} + i\varepsilon)^{-1}$ in coordinate space, where \hat{x} is the position operator. We obtain

$$\begin{aligned}
F(x_1, x_2) &= \frac{1}{\pi^2} \lim_{\varepsilon \rightarrow 0^+} \sum_{i,j=1}^N \text{Im} \langle \phi_i | \hat{G}(x_1) | \phi_j \rangle \text{Im} \langle \phi_j | \hat{G}(x_2) | \phi_i \rangle \\
&= \frac{1}{\pi^2} \lim_{\varepsilon \rightarrow 0^+} \text{Tr} \left\{ \text{Im} \left[\hat{G}_N(x_1) \right] \cdot \text{Im} \left[\hat{G}_N(x_2) \right] \right\}, \tag{23}
\end{aligned}$$

where $|\phi_i\rangle$ are the eigenstates of the 1D Hamiltonian in the coordinate representation and $\hat{G}_N(x)$ is the first $N \times N$ block of the matrix $\hat{G}(x)$. We then use the property $\text{Im}A \cdot \text{Im}B = (1/2)[\text{Re}(A \cdot B^*) - \text{Re}(A \cdot B)]$ to obtain

$$F(x_1, x_2) = \frac{1}{2\pi^2} \lim_{\varepsilon \rightarrow 0^+} \left\{ \text{ReTr} \left[\hat{G}_N(x_1) \cdot \hat{G}_N^*(x_2) \right] - \text{ReTr} \left[\hat{G}_N(x_1) \cdot \hat{G}_N(x_2) \right] \right\}. \tag{24}$$

We can now use the relation $\text{Tr} Q^{-1} = [\partial \log \det(Q + \lambda \mathbb{I}) / \partial \lambda]_{\lambda=0}$ [16], with \mathbb{I} being the identity matrix $N \times N$, to obtain the final expression

$$\begin{aligned}
F(x_1, x_2) &= \frac{1}{2\pi^2} \lim_{\varepsilon \rightarrow 0^+} \text{Re} \frac{\partial}{\partial \lambda} \left[\log \det \left((x_2 - \hat{\xi}^*(x_2) - i\varepsilon) \cdot (x_1 - \hat{\xi}(x_1) + i\varepsilon) + \lambda \mathbb{I} \right) \right]_{\lambda=0} \\
&\quad - \frac{1}{2\pi^2} \lim_{\varepsilon \rightarrow 0^+} \text{Re} \frac{\partial}{\partial \lambda} \left[\log \det \left((x_2 - \hat{\xi}(x_2) + i\varepsilon) \cdot (x_1 - \hat{\xi}(x_1) + i\varepsilon) + \lambda \mathbb{I} \right) \right]_{\lambda=0}. \tag{25}
\end{aligned}$$

Here, $\hat{\xi}(x)$ is a renormalized position operator [17], reduced to the $N \times N$ subspace.

While Eq. (25) holds for any 1D confining potential, this approach is particularly useful for the case of harmonic confinement where the representation of the position operator is tridiagonal. In this case the renormalized operator $\hat{\xi}(x)$ reads $[\hat{\xi}(x)]_{i,j} = [\hat{x}]_{i,j}$ if $(i, j) \neq (N, N)$ and $[\hat{\xi}(x)]_{N,N} = \tilde{x}_{N,N}(x)$, with

$$\tilde{x}_{N,N}(x) = \frac{N/2}{x + i\varepsilon - \frac{(N+1)/2}{x + i\varepsilon - \dots}}. \tag{26}$$

The evaluation of $F(x_1, x_2)$ is thus reduced to the calculation of the determinant of pentadiagonal $N \times N$ matrices. If we make a partition into blocks A_i and $B_{i,j}$ of dimension 2×2 , a pentadiagonal matrix Q takes a tridiagonal form. For even N we can write (see also [11])

$$Q = \begin{pmatrix} A_1 & B_{1,2} & & & \\ B_{2,1} & A_2 & B_{2,3} & & \\ & B_{3,2} & \ddots & \ddots & \\ & & \ddots & \ddots & A_{N/2} \end{pmatrix}, \tag{27}$$

and the determinant of such a matrix can be factorizes into the product of 2×2 matrices as

$$\det Q = \prod_i \det \tilde{A}_i. \tag{28}$$

Here, $\tilde{A}_1 = A_1$ and $\tilde{A}_i = A_i - B_{i,i-1}(\tilde{A}_{i-1})^{-1}B_{i-1,i}$ for $i > 1$. If N is odd we obtain an analogous expression in which the last block of the partition is a 1×1 matrix.

B. Numerical results

By the method outlined above we have calculated the longitudinal contribution to the equal-times pair distribution function, $\rho_2^{(l)}(x_1, x_2) = n(x_1)n(x_2) - F(x_1, x_2)$, for up to $N = 100$ fermions without particular numerical efforts. Since this function presents in general a number of maxima of order N^2 , for the sake of clarity we have shown in Fig. 5 the full result only for the case of $N = 4$ fermions.

The numerical results for higher values of the particle number N are shown in Fig. 6 through a section of the pair distribution function taken at the value $R \equiv (x_1 + x_2)/2 = 0$ of the center-of-mass coordinate. In the confined gas the effect of Pauli exclusion is also observable in real space as a depression of $\rho_2^{(l)}(x_1, x_2)$ at short distance $r \equiv (x_1 - x_2)$. This is more clearly illustrated in the inset of Fig. 6 through an enlargement of the region near $r = 0$. At larger distances the function $F(x_1, x_2)$ goes rapidly to zero and the pair function decouples into the product of two particle density profiles. For other sections of the pair function a similar behavior is found with a reduced number of peaks in the profile. This is shown in Fig. 7 for the illustrative case of $N = 4$ fermions.

VII. SUMMARY AND CONCLUSIONS

In summary, we have evaluated the scattering functions of quasi-1D mesoscopic clouds of non-interacting fermions in an external harmonic potential. A number of conclusions can be drawn from our results.

The inelastic scattering spectrum of the inhomogeneous gas, displayed in Fig. 2, reflects its restricted geometry through (i) the form factor coming from the tight transverse confinement, and (ii) its general shape, which is remarkably different from that of the homogeneous gas, as can be predicted already in a local-density calculation (see Eqs. (12)-(15)). In principle the spectral intensity has a discrete structure owing to the level spacings induced by the axial confinement, but this spectral structure is rapidly smoothed away as the number N of fermions in the cloud increases.

The elastic contribution to the scattering cross section is dominated by the main peak centered at zero momentum transfer and broadened as a consequence of the finite axial size of the cloud (see Fig. 3 (a)). The shell structure of the cloud appears in the elastic scattering intensity only as an extremely weak peak located at momentum transfer close to twice the Fermi momentum. This peak lies in the far tail of the central elastic peak (see Fig. 3 (b)) and will be masked by the inelastic scattering contribution to the diffraction pattern.

The inelastic contribution to the static structure factor in Fig. 4 is obtained by integration of the dynamic structure factor over energy transfers. Similar comments apply, therefore, to these two scattering functions: thus, $S_i(k_x)$ is clearly reflecting the shell structure of the cloud only for limited values of the number of fermions (see the inset of Fig. 4). The general shape of $S_i(k_x)$ in the main body of Fig. 4 is again related through the local-density scheme to the static structure factor of the 1D Fermi gas.

The equal-times pair distribution function contains a much greater and detailed amount of information on the relative spatial distribution of pairs of particles in the inhomogeneous Fermi gas. Here it is, of course, a function both of the relative distance r of the pair and of the coordinate R of its center-of-mass along the x axis. The Pauli “exchange” hole surrounding each fermion is a well-known feature of the pair distribution function in homogeneous Fermi gases and is a very prominent feature in the spin-polarized inhomogeneous system. It is seen in Fig. 5 as the deep valley running in a direction parallel to the R axis and cutting into two separate parts the contour plot at $r = 0$. It is again seen in the inset of Fig. 6 at $R = 0$ and in Fig. 7 at various values of R . In addition to this basic feature, the two-body distribution displays a great deal of secondary structures, of order N^2 as already noted, which descend from the combination of the Pauli principle and of the axial confinement.

In conclusion, the single occupancy of the discrete quantum levels in the quasi-1D Fermi gas may become accessible in light scattering experiments by looking at the inelastic scattering spectrum. It also affects to some extent the angular distribution of the inelastically scattered light. The elastic contribution to the scattering is quite negligible in this respect.

ACKNOWLEDGMENTS

A.M. acknowledges useful discussions with Dr. I. Carusotto. This work was partially supported by MURST under the PRIN2000 Initiative.

-
- [1] B. DeMarco and D. S. Jin, *Science* **285**, 1703 (1999); M. J. Holland, B. DeMarco, and D. S. Jin, *Phys. Rev. A* **61**, 053610 (2000).
 - [2] M. O. Mewes, G. Ferrari, F. Schreck, A. Sinatra, and C. Salomon, *Phys. Rev. A* **61**, 011403(R) (2000); F. Schreck, G. Ferrari, K. L. Corwin, G. Cubizolles, L. Khyakovich, M. O. Mewes, and C. Salomon, *cond-mat/0011291*.
 - [3] B. DeMarco and D. S. Jin, *Phys. Rev. A* **58**, R4267 (1998).
 - [4] H. T. C. Stoof and M. Houbiers, in *Bose-Einstein Condensation in Atomic Gases*, eds. M. Inguscio, S. Stringari and C. E. Wieman (IOS Press, Amsterdam, 1999), p. 537.
 - [5] M. D. Girardeau, *Journ. Math. Phys.* **1**, 516 (1960); M. D. Girardeau and E. M. Wright, *Phys. Rev. Lett.* **84**, 5239 (2000); E. B. Kolomeisky, T. J. Newman, J. P. Straley, and X. Qi, *ibid.* **85**, 1146 (2000).
 - [6] See, for instance S. Lundqvist and N. H. March, *Theory of the Inhomogeneous Electron Gas* (Plenum, New York, 1983); R. G. Parr and W. Yang *Density Functional Theory of Atoms and Molecules* (University Press, Oxford, 1989); E. K. Gross, J. F. Dobson, and M. Petersilka, in *Topics in Current Chemistry*, ed. R. F. Nalewejski (Springer, Berlin, 1996), p. 1.

- [7] G. P. Lawes and N. H. March, *J. Chem. Phys.* **71**, 1007 (1979); A. Minguzzi, N. H. March, and M. P. Tosi, *cond-mat/0102186*
- [8] J. Schneider and H. Wallis, *Phys. Rev. A* **57**, 1253 (1998); G. M. Bruun and K. Burnett, *ibid.* **58**, 2427 (1998).
- [9] P. Vignolo, A. Minguzzi, and M. P. Tosi, *Phys. Rev. Lett.* **85**, 2850 (2000).
- [10] F. Gleisberg, W. Wonneberger, U. Schlöder and C. Zimmermann, *Phys. Rev. A* **62**, 063602 (2000).
- [11] A. Minguzzi, P. Vignolo, and M. P. Tosi, *cond-mat/0011331*.
- [12] D. Pines and P. Nozières, *The Theory of Quantum Liquids*, (W. A. Benjamin, New York, 1966) Vol. I.
- [13] J. Javanainen and J. Ruostekoski, *Phys. Rev. A* **52**, 3033 (1995).
- [14] I. S. Gradshteyn and I. M. Ryzhik, *Table of Integrals, Series and Products, Corrected and Enlarged Edition*, (Academic, San Diego, 1980), Eq. 7.377.
- [15] M.D. Girardeau, E. M. Wright, and J. M. Triscari, *Phys. Rev. A* **63**, 033601 (2001).
- [16] R. Farchioni, G. Grosso, and P. Vignolo, *Phys. Rev. B* **62**, 12565 (2000).
- [17] For the use of renormalized operators see for instance G. Grosso and G. Pastori Parravicini, *Solid State Physics* (Academic, London 2000) p. 191.

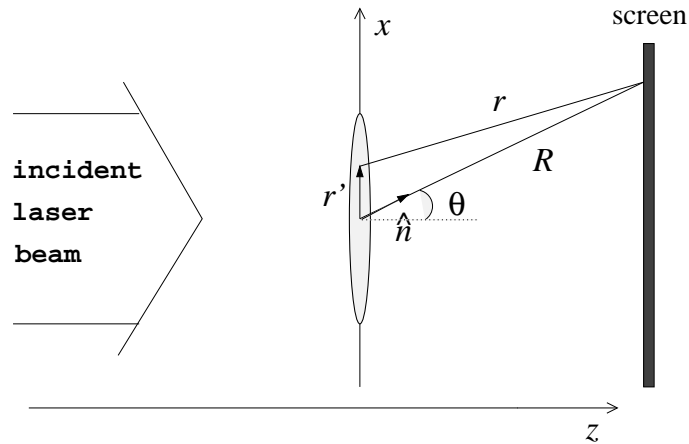


FIG. 1. Geometry of the light scattering configuration described in the text.

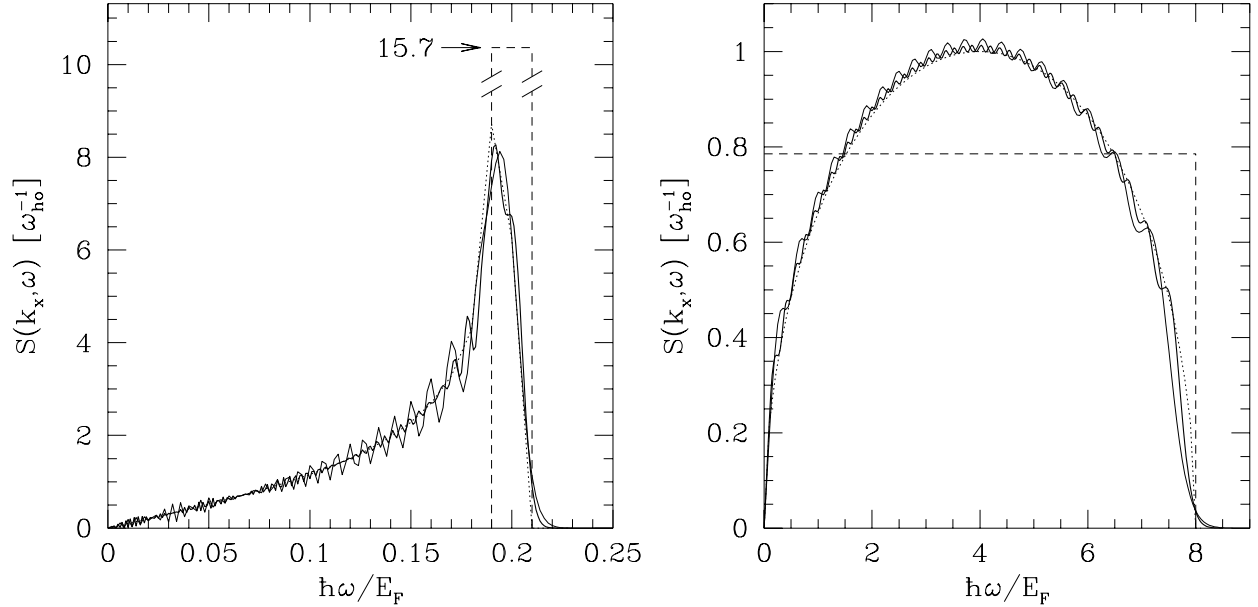


FIG. 2. Dynamic structure factor $S(k_x, \omega)$ of a 1D harmonically confined Fermi gas (in units of ω_{ho}^{-1}) as a function of $\hbar\omega/E_F$, where $E_F = N\hbar\omega_{ho}$. Left panel: at $k_x = 0.1 k_F$ and numbers of fermions $N=500$ (solid line) and $N=1000$ (solid bold line). Right panel: at $k_x = 2 k_F$ and $N=20$ (solid line) and $N=40$ (solid bold line). In both panels the LDA spectrum (dotted line) and the dynamic structure factor of a homogeneous 1D Fermi gas (dashed line) are plotted in the same units. The exact $S(k_x, \omega)$ is shown for clarity as constructed from discrete frequencies by joining vertical lines having height proportional to the oscillator strength.

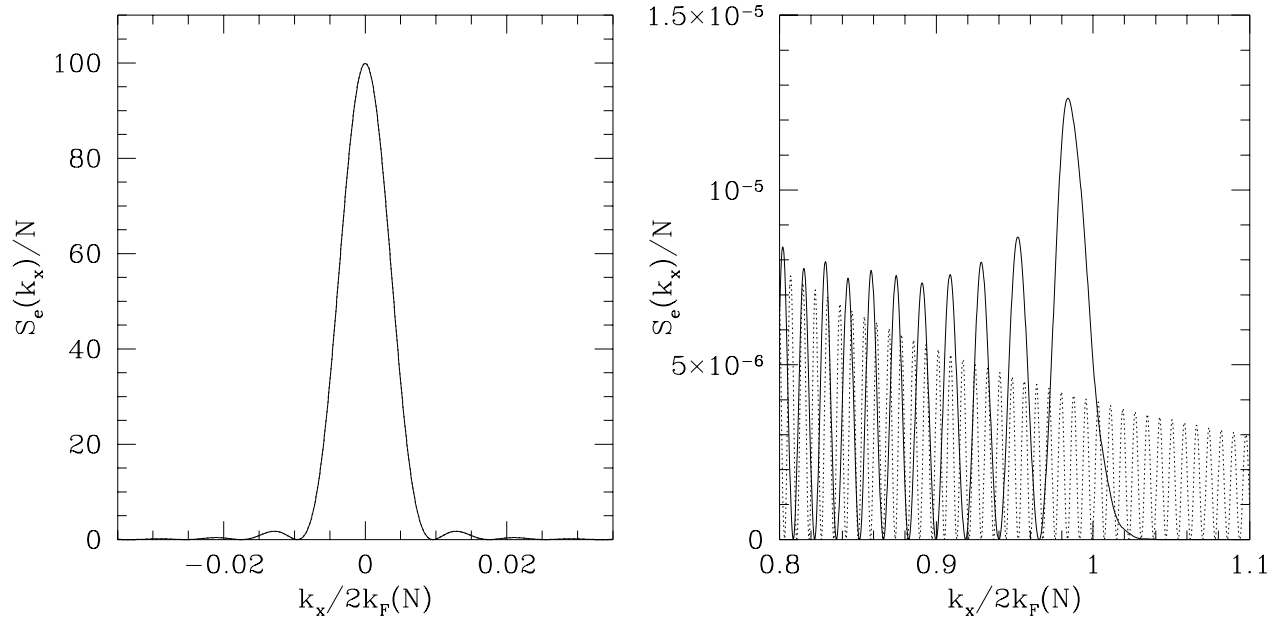


FIG. 3. Central peak (left panel) and side peak (right panel) of the elastic contribution to the static structure factor, normalized to $N = 100$ fermions, as a function of the wave number k_x (in units of $2k_F(N) = 2\sqrt{2N} a_{ho}^{-1}$) at fixed $k_\perp = 0$. Both the true profile (continuous line) and the LDA profile (dotted line) are shown.

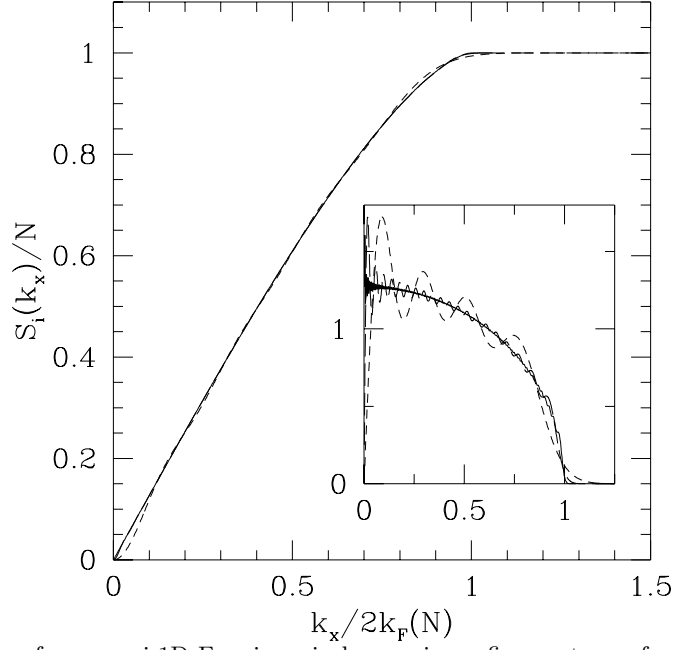


FIG. 4. Static structure factor for a quasi-1D Fermi gas in harmonic confinement as a function of the wave number k_x (in units of $2k_F(N)$) at $k_\perp = 0$. The inset shows the first derivative of $S_i(k_x)$ in the same reduced units. The numbers of fermions are $N = 4$ (short-dashed line), $N = 20$ (long-dashed line) and $N = 100$ (solid line).

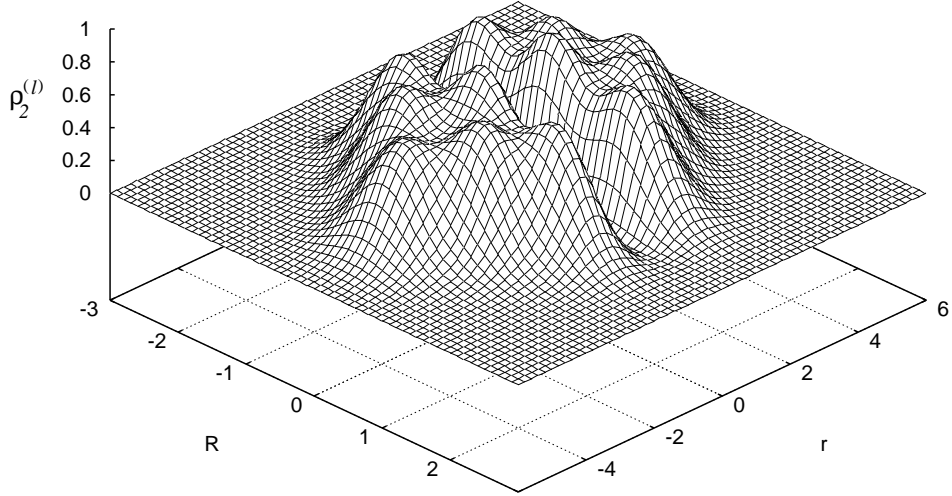


FIG. 5. Longitudinal contribution $\rho_2^{(l)}(r; R)$ to the pair distribution function for $N=4$ fermions in quasi-1D harmonic confinement, in units of a_{ho}^{-2} , as a function of the center-of-mass coordinate R and of the relative coordinate r , both in units of a_{ho} .

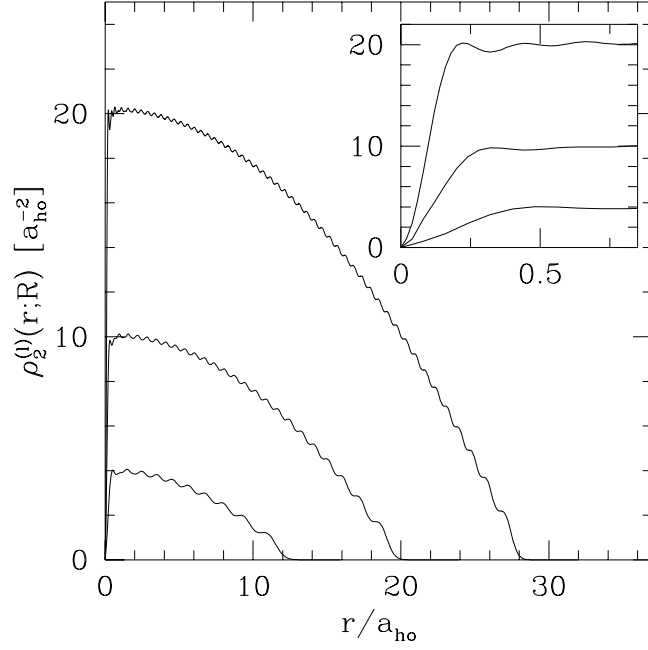


FIG. 6. Section of $\rho_2^{(l)}(r;R)$ at $R=0$ for $N=20, 50$ and 100 fermions at $R=0$ (from bottom to top), in units of a_{ho}^{-2} , as a function of the relative coordinate r/a_{ho} of the pair. The inset shows an enlargement of the region near $r=0$, in the same units.

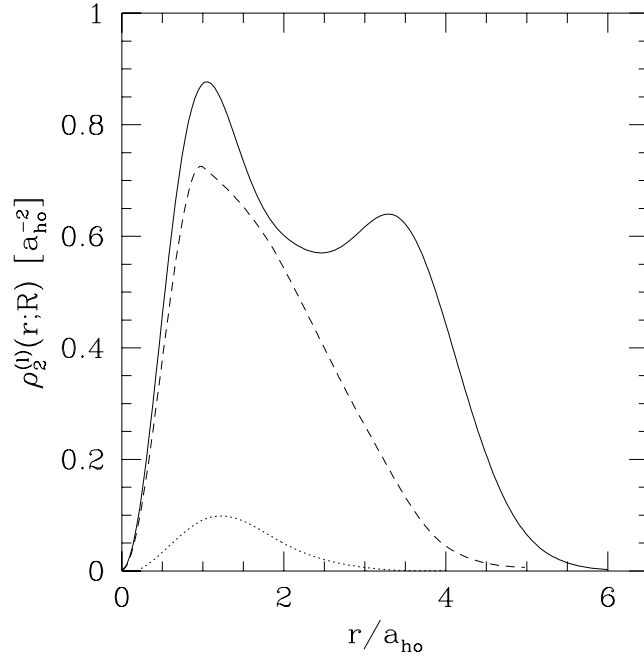


FIG. 7. Sections of $\rho_2^{(l)}(r;R)$ for values of $R=0$ (solid line), $R=a_{ho}$ (dashed line) and $R=2a_{ho}$ (dotted line) at $N=4$. Notations and units are as in Fig. 6.